

## NONLINEAR SEISMIC ANALYSIS OF A CANDU CONTAINMENT STRUCTURE SUBJECTED TO SCENARIO EARTHQUAKES

**In-Kil Choi**

*Principal Researcher, Korea Atomic  
Energy Research Institute, Korea*  
Phone: 82-42-868-2056  
E-mail: cik@kaeri.re.kr

**Jeong-Moon Seo**

*Principal Researcher, Korea Atomic  
Energy Research Institute, Korea*  
Phone: 82-42-868-8371  
E-mail: jmseo@kaeri.re.kr

**Young-Sun Choun**

*Principal Researcher, Korea Atomic  
Energy Research Institute, Korea*  
Phone: 82-42-868-2036  
E-mail: sunchun@kaeri.re.kr

**Seong-Moon Ahn**

*Researcher, Korea Atomic Energy  
Research Institute, Korea*  
Phone: 82-42-868-8132  
E-mail: ex-saymoon@kaeri.re.kr

### ABSTRACT

In this study, the seismic safety of a CANDU containment structure is estimated by performing the nonlinear seismic analysis for the scenario earthquakes. The lumped mass model of the containment building was developed for a nonlinear dynamic time history analysis. The tri-linear skeleton curve was used for the nonlinear behavior of the prestressed concrete containment building. In order to estimate the inelastic nonlinear response of the containment, the maximum point oriented model was used for the hysteretic rule of the shear deformation.

Three kinds of earthquake ground motions which represent the design earthquake ground motion for the Korean nuclear power plants, the probability based scenario earthquakes for the Korean nuclear power plant sites and the 30 set of real near-fault earthquake records were used as the input motion. The seismic response of the containment for the design earthquake is compared with the responses for the probability based scenario earthquake and the near-fault earthquake record. The floor response of the structure was estimated to evaluate the seismic safety of the safety related equipment installed in the building.

**Keywords:** CANDU Containment, Nonlinear Dynamic Analysis, Seismic Safety, Scenario Earthquakes

### 1. INTRODUCTION

The standard response spectrum (NRC, 1973) proposed by US NRC has been used as a design earthquake for the design of Korean nuclear power plant structures. However the seismic safety of a nuclear power plant can not be secured by considering only the design basis earthquake, since the seismological situation of the nuclear power plant site is changed during the development of geosciences. The probabilistic seismic hazard analyses (PSHA) for the Korean nuclear power plant sites were performed as a part of the probabilistic seismic safety assessment. It is possible to estimate the site-dependent design earthquake and the uniform hazard response spectra for a given exceedance probability. In Korea, a survey on some of the Quaternary fault segments near Korean nuclear power plants is ongoing (KINS, 2000). It is likely that these faults will be identified as active ones. If the faults are confirmed as active ones, it will be necessary to reevaluate the seismic safety of the nuclear power plants located near the faults.

Near-fault ground motions are the ground motions that occur near an earthquake fault. In general, the near-fault ground motion records exhibit a distinctive long period pulse like time history with very high peak

velocities. These features are induced by the slip of the earthquake fault. Near-fault ground motions, which have caused much of the damage in recent major earthquakes, can be characterized by a pulse-like motion that exposes the structure to a high input energy at the beginning of the motion. Some Quaternary fault systems being surveyed are located near the nuclear power plants.

In this study, nonlinear dynamic time-history analyses were performed to investigate the seismic behavior of a CANDU containment structure subjected to various earthquake ground motions including the near-field ground motions.

## 2. SCENARIO EARTHQUAKES

In this study, three kinds of scenario earthquakes were defined as input ground motions for the seismic analyses. The first one is the standard response spectrum proposed by U.S. NRC Regulatory 1.60, which is a design response spectrum for most Korean nuclear power plants. The second one is the PBSE based on the PSHA. The probability based scenario earthquakes (PBSE) for a Korean NPP site were developed using the method proposed by the U.S. NRC Regulatory Guide 1.165 (NRC, 1997). The seismic hazard was de-aggregated to determine the dominant magnitudes and distances at the prescribed exceedance level. In this study, the seismic hazard was de-aggregated at a  $10^{-5}$  exceedance level according to the U.S. NRC Regulatory Guide 1.165 (NRC, 1997). The spectral shape for the PBSE was developed using the attenuation equations proposed in the PSHA study [4]. The features of the near-fault ground motion were considered in the spectral shape of the PBSE by using the method proposed by Ohno et al. (1998). Ohno et al. (1998) showed the range at which the near-fault rupture directivity effect is dominant and proposed a method to correct the predefined response spectrum by considering this effect. The last one is 30 sets of near-fault ground motion records which had occurred in the world.

These three kinds of scenario earthquakes were used as input ground motion for the nonlinear seismic analysis of the CANDU containment building to estimate the seismic behavior for various earthquake ground motions.

## 3. MODELING OF THE CANDU CONTAINMENT BUILDING

### 3.1 Characteristics of CANDU Containment Building

The containment type of a CANDU nuclear power plant is not tied to the design. The CANDU containment building in Korea, which houses the nuclear reactor and safety related equipments, is a prestressed, post tensioned reinforced concrete structure (CANATOM, 1994). Fig. 1 shows the schematic view of a CANDU containment building. The CANDU containment consists of a base slab, perimeter wall, ring beam and upper dome. The containment building of CANDU nuclear power plant has some specific features, such as a dousing tank, dousing frame, ring beam, etc., when compare with that of the PWR plant. The CANDU containment contains the dousing water of  $1,560\text{m}^3$  in an elevated tank around the building dome for powerful pressure suppression, not like the PWR sprays.

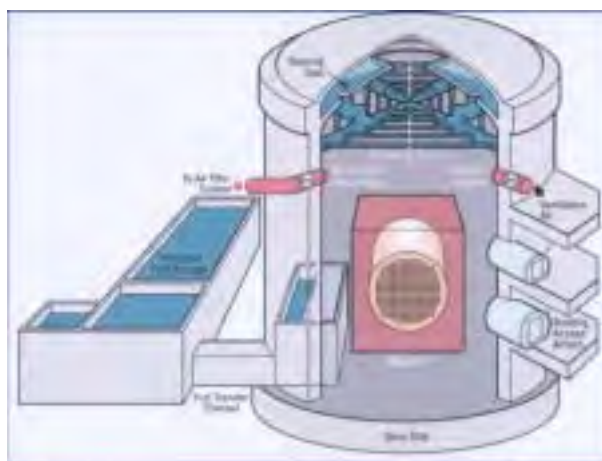


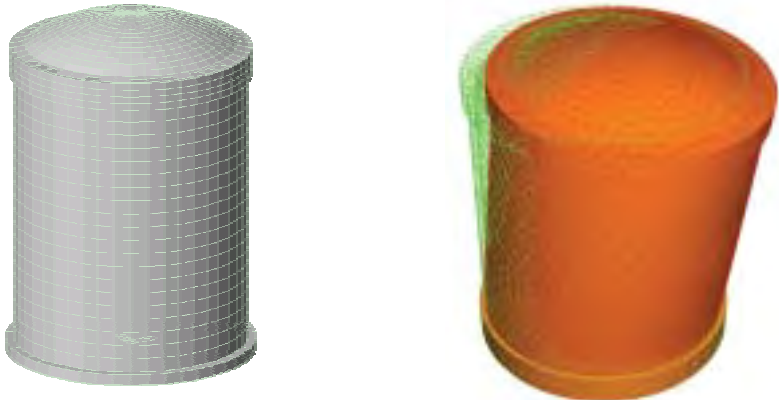
*Fig. 1 CANDU Containment Building*

### 3.2 Analysis Model

A three dimensional finite element model was used for the eigenvalue analysis of the CANDU containment building. Fig. 2 (a) shows the three dimensional finite element model. Fig. 2 (b) shows the fundamental frequency

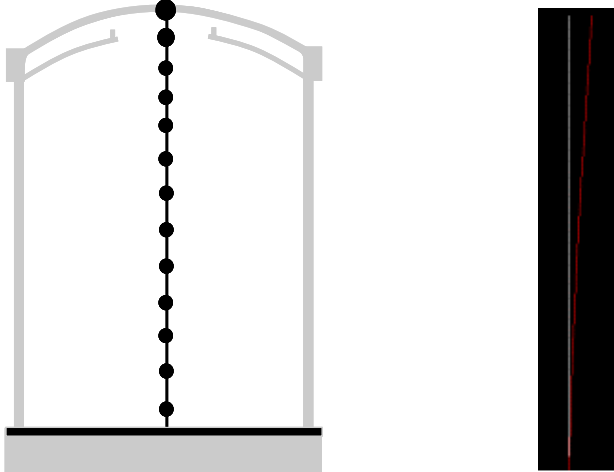
and mode shape. As shown in this figure, the fundamental frequency of a CANDU containment building is 3.86 Hz. This natural frequency coincides very well with the natural frequency, 3.80 Hz for a hard rock condition, reported in the design report of the Wolsung-2 nuclear power plant (CANATOM, 1994).

A lumped mass model was developed for the nonlinear dynamic time history analysis. The mass of the dousing water was assumed to be attached to the adjacent parts of the domes and the ring beams in each of the analysis model. Figure 3 shows the lumped mass model for the containment building and its fundamental mode shape with the fundamental frequency. The fundamental frequencies of the containment building by the 3-D FE model and the lumped mass model were 3.86 Hz and 3.84 Hz, respectively. This result shows that the lumped mass model can be used to approximate the 3-D FE model for the nonlinear dynamic time history analysis.



(a) 3-D FEM Model      (b) Fundamental Mode Shape (3.86Hz)

Fig. 2 3-D Finite Element Model of the CANDU Containment Building and Fundamental Mode Shape



(a) Lumped Mass Model      (b) Fundamental Mode Shape (3.84Hz)

Fig. 3 Lumped Mass Model for the Nonlinear Dynamic Analysis and Its Fundamental Mode Shape

**3.3 Nonlinear Hysteretic Model**

In this study, the tri-linear approximation shown in figure 4 was used for the shear behavior of the containment building. The turning points for the shear stress and strain relationship were determined based on the EPJR (Electric Power Joint Research) method (Park et al., 1994). In order to perform the elasto-plastic seismic response analysis, based on the tri-linear skeleton curve, the maximum point oriented model was used as the hysteresis rule for the repeated unloading and loading processes. Figure 5 shows the hysteresis rule of the maximum point oriented model. The moment-curvature relationship is assumed as linear elastic, since the containment building is a very thick reinforced concrete structure and its dominant failure is a shear failure at the

bottom of the containment shell.

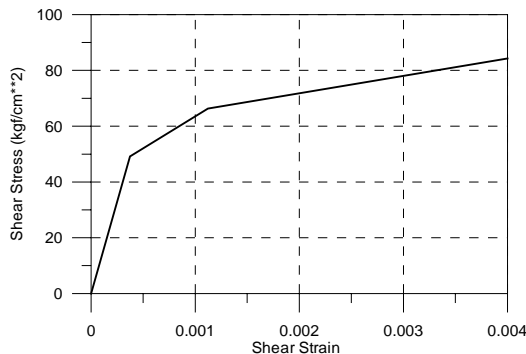


Fig. 4 Tri-linear Skeleton Curve

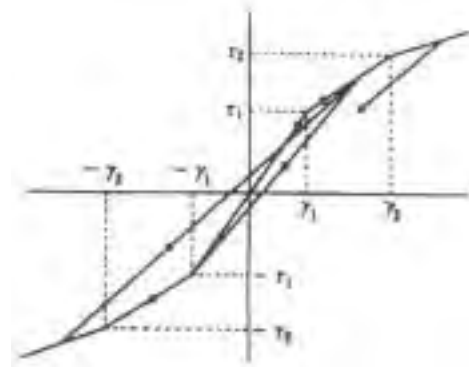


Fig. 5 Maximum Point-oriented Model

#### 4. NONLINEAR SEISMIC ANALYSIS

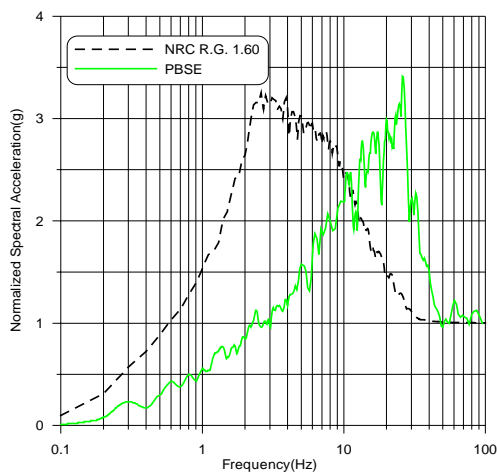
##### 4.1 Input Motions

Three types of input motions, artificial time histories that envelop the US NRC Regulatory Guide 1.60 spectrum (NRC, 1993) and the probability based scenario earthquake (Choi et al., 2003), and several near-field earthquake records were used for the seismic analyses. Figure 6 (a) shows the NRC and PBSE spectrum. The ground response spectrum of the PBSE is determined by using the ground motion attenuation equations used in the PSHA study (Seo et al., 1999). As can be seen in this figure, the two input earthquakes have very different frequency contents. The PBSE spectrum shows that the amplification in the high frequency range is very high. Figure 6 (b) shows the ground response spectra of the 30 set of near-fault ground motions used in this study. The near-fault earthquake records used for the seismic analysis are listed in Table 1. The characteristics of these earthquake records are also summarized in this table. Figure 7 shows the generated artificial acceleration time histories that envelop the NRC and PBSE ground response spectra. The artificial acceleration time histories were generated by using the SIMQKE program (Vanmarcke et al., 1976).

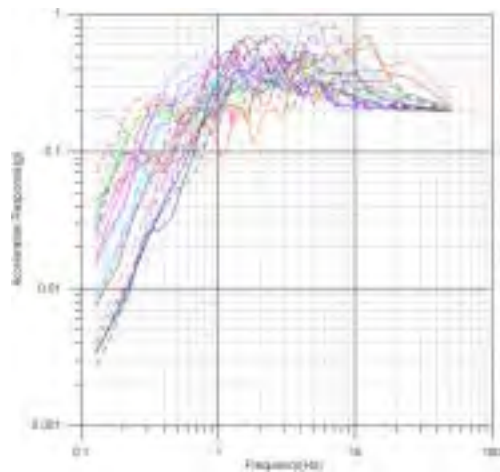
Table 1. Near Fault Ground Motions Used for the Seismic Analysis

Earthquake	Date	Station	Closest to Fault Rupture (km)	Closest to Surface Projection of Rupture(km)	Magnitude	PGA (g)	PGV (cm/sec)
Coyote Lake	1979-08-06	57383 Gilroy Array#6	3.10	1.20	5.7	0.434	49.2
Duzce, Turkey	1999-11-12	Duzce	8.20	8.20	7.1	0.535	83.5
Erzincan, Turkey	1992-03-13	95 Erzincan	2.00	-	6.9	0.515	83.9
Gazli, USSR	1976-05-17	9201 Karakyr	-	-	6.8	0.608	65.4
Imperial Valley	1979-10-15	955 El Centro Array #4	4.20	6.80	6.5	0.360	76.6
Imperial Valley	1979-10-15	952 El Centro Array #5	1.00	4.00	6.5	0.379	90.5
Imperial Valley	1979-10-15	942 El Centro Array #6	1.00	1.30	6.5	0.439	109.8
Kobe	1995-01-16	0 Takarazuka	1.20	-	6.9	0.694	85.3
Kocaeli, Turkey	1999-08-17	Arcelik	17.00	17.00	7.4	0.149	39.5
Kocaeli, Turkey	1999-08-17	Sakarya	3.10	3.10	7.4	0.376	79.5
Kocaeli, Turkey	1999-08-17	Yarimca	2.60	2.60	7.4	0.268	65.7
Landers	1992-06-28	24 Lucerne	1.10	-	7.3	0.721	97.6
Loma Prieta	1989-10-18	16 LGPC	6.10	-	6.9	0.605	51.0
Loma Prieta	1989-10-18	58065 Saratoga - Aloha Ave	13.00	11.70	6.9	0.324	42.6
Morgan Hill	1984-04-24	57191 Halls Valley	3.40	-	6.2	0.312	39.4

N.Palm Springs	1986-07-08	12149 Desert Hot Springs	8.00	-	6.0	0.331	29.5
N.Palm Springs	1986-07-08	5070 North Palm Springs	8.20	-	6.0	0.594	73.3
Northridge	1994-01-17	0655 Jensen Filter Plant	6.20	-	6.7	0.424	106.2
Northridge	1994-01-17	77 Rinaldi Receiving Sta	7.10	-	6.7	0.838	166.1
Northridge	1994-01-17	74 Sylmar - Converter Sta	6.20	0.20	6.7	0.612	117.4
Parkfield	1966-06-28	1013 Cholame #2	0.10	6.60	6.1	0.476	75.1
San Fernando	1971-02-09	279 Pacoima Dam	2.80	-	6.6	1.226	112.5
SuperStition Hills	1987-11-24	01335 El Centro Imp. Co. Cent	13.90	-	6.7	0.358	46.4
SuperStition Hills	1987-11-24	5051 Parachute Test Site	0.70	-	6.7	0.455	112.0
Tabas, Iran	1978-09-16	9101 Tabas	-	-	7.4	0.852	121.4
Whittier Narrows	1987-10-01	14368 Downey - Co Maint Bldg	18.30	-	6.0	0.221	28.8
Whittier Narrows	1987-10-01	634 Norwalk - Imp Hwy, S Grnd	17.10	-	6.0	0.248	20.7
Chi-Chi, Taibei	1999-09-20	TCU052	0.24	0.06	7.6	0.419	118.4
Chi-Chi, Taibei	1999-09-20	TCU068	1.09	0.50	7.6	0.462	263.1
Chi-Chi, Taibei	1999-09-20	TCU075	1.49	1.49	7.6	0.333	88.3

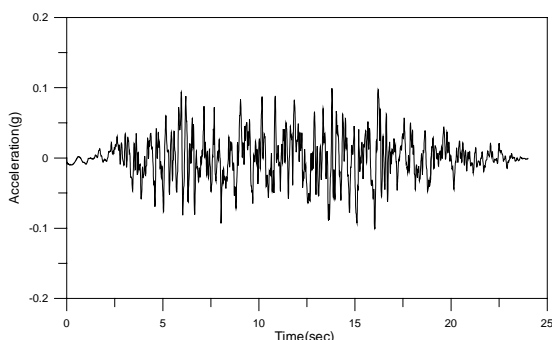


(a) NRC RG 1.60 and PBSE

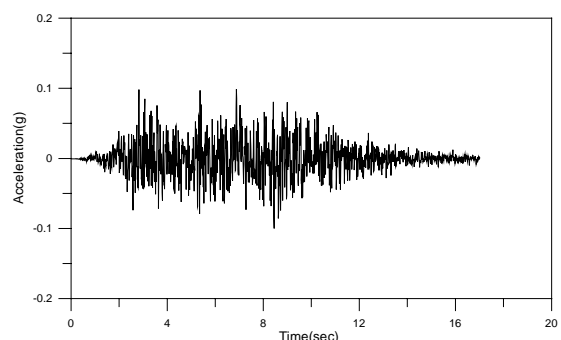


(b) Near-Fault Earthquakes

Fig. 6 Acceleration Response Spectra of Input Motions



(a) NRC RG 1.60



(b) PBSE

Fig. 7 Generated Artificial Acceleration Time Histories

#### 4.2 Response of Containment Building

The nonlinear inelastic dynamic analyses of the containment building were performed to investigate the

seismic response for the input ground motions. In the design stage, the elastic analysis was performed to obtain the member stress and floor acceleration. The response spectrum analysis method is generally used for the seismic design of a NPP containment building. Figure 8 shows the maximum displacement response of the containment building at the top according to the peak ground acceleration (PGA) of the near fault ground motions. The solid line represents the mean response. The containment building shows a linear elastic behavior up to 1.2g PGA. Figure 9 shows the comparison of the maximum displacement response for various input ground motions. The maximum displacement response is rapidly increased from 0.8g PAG for the NRC ground motion due to the nonlinear response. Figure 10 shows the shear force – displacement relationship at the bottom of the containment building at 2.0g PGA. It definitely shows an inelastic nonlinear response.

Figure 11 shows the maximum acceleration response at the top for the scenario earthquakes. As shown in this figure, the maximum acceleration responses due to the NRC ground motion are larger than those due to the PBSE and mean responses of the near fault ground motions. The containment building shows a nonlinear response to a NRC ground motion greater than 0.8g PGA. The maximum acceleration response is linearly increased up to 1.8g PGA. In contrast to the displacement response, the acceleration response was decreased in comparison to the elastic response.

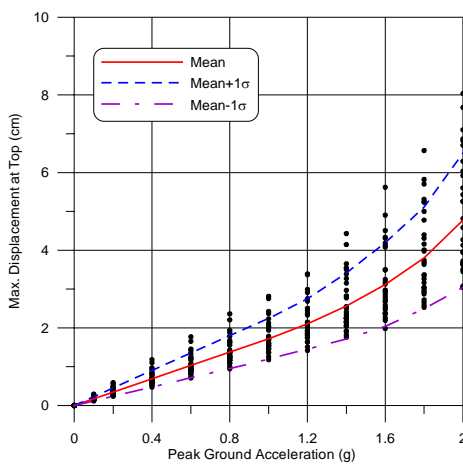


Fig. 8 Maximum Top Displacement for Near-Fault Ground Motions

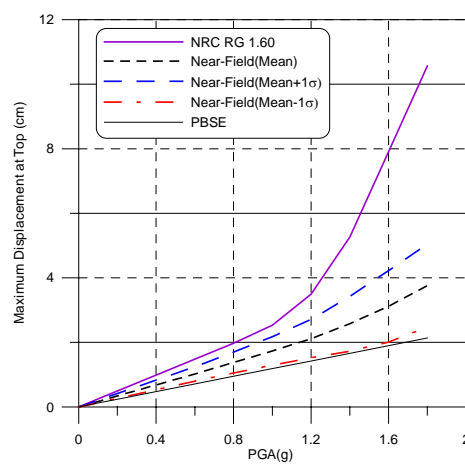


Fig. 9 Comparison of Maximum Top Displacement

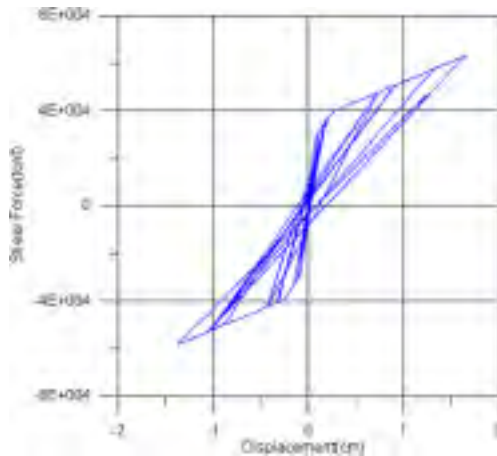


Fig. 10 Hysteretic Behavior of Containment Building

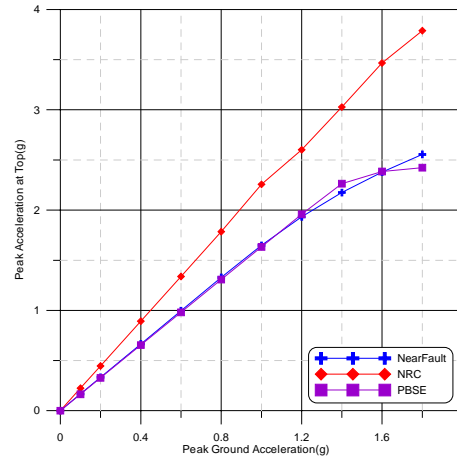


Fig. 11 Peak Acceleration at Top

Figure 12 shows the maximum shear force at the bottom according to the increase of the PGA for the scenario earthquakes. The shear force due to the PBSE is smaller than those due to other ground motions. From this figure, it can be known that the acceleration response due to the PBSE is similar to that due to the near fault ground motions, but the shear force is small because of the frequency contents of the PBSE ground motion. It means that the acceleration response can be greatly amplified for the high frequency ground motions, but the high frequency ground motion dose not damage the containment building.

In figure 13, the maximum shear force response from the nonlinear inelastic response analysis for the NRC ground motion is compared with that from the linear elastic analysis. The right ordinate of this figure represents the response ratio of the linear elastic response to the nonlinear inelastic response. The maximum shear force from the linear analysis at 1.8g is 1.3 times that from nonlinear analysis.

Figure 14 shows the normalized maximum displacement and shear force ratio for the linear elastic response. It is known from figure 14 (a) that the displacement response from the nonlinear analysis for the PBSE is similar to that from the linear analysis. It means that the containment behaves linearly for the PBSE up to 1.8g. The maximum displacement response is increased rapidly for the NRC ground motion. The displacement ratio is increased up to 2.3 at 1.8g PGA. The displacement ratio for the near fault ground motion is not so great. Figure 14 (b) shows the normalized maximum shear force ratio for the linear elastic response. The maximum shear force is greatly reduced due to the nonlinear response of the containment building. In this figure, it can be easily known whether the containment behaves in the linear elastic range or not at a certain PGA level. The containment shows a nonlinear response from 0.6g PGA for the NRC ground motion and the near fault ground motions. And the containment shows nonlinear response from the 1.2 PGA level for the PBSE.

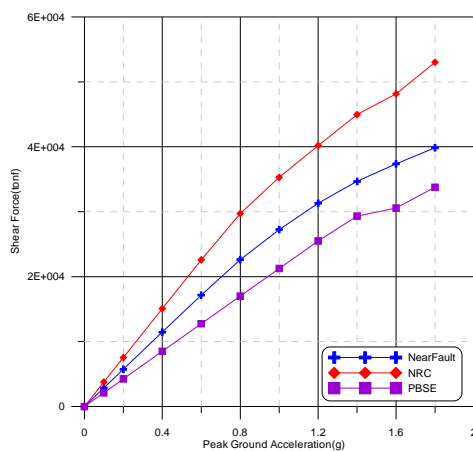


Fig. 12 Maximum Shear Force

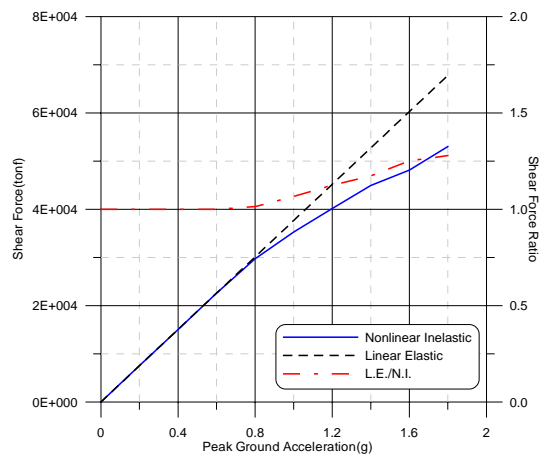
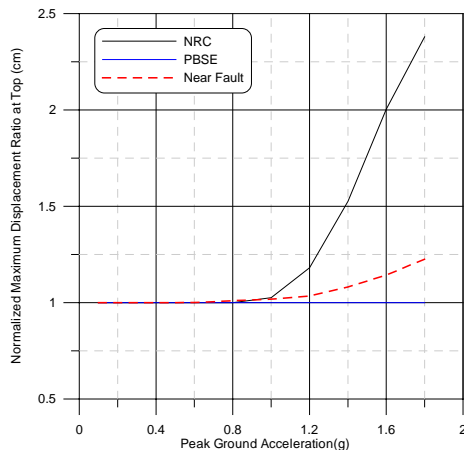
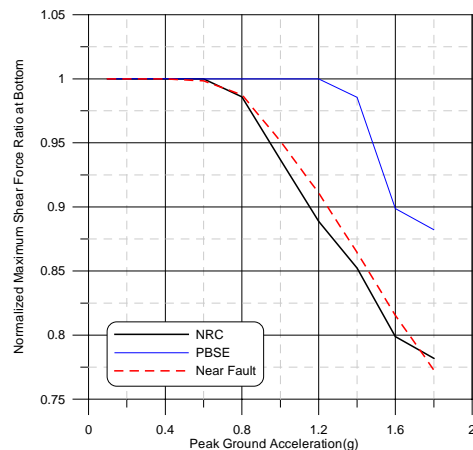


Fig. 13 Comparison of Maximum Shear Forces



(a) Maximum Displacement at Top



(b) Maximum Shear Force at Bottom

Fig. 14 Normalized Response Ratios to the Linear Elastic Response

### 4.3 Floor Response

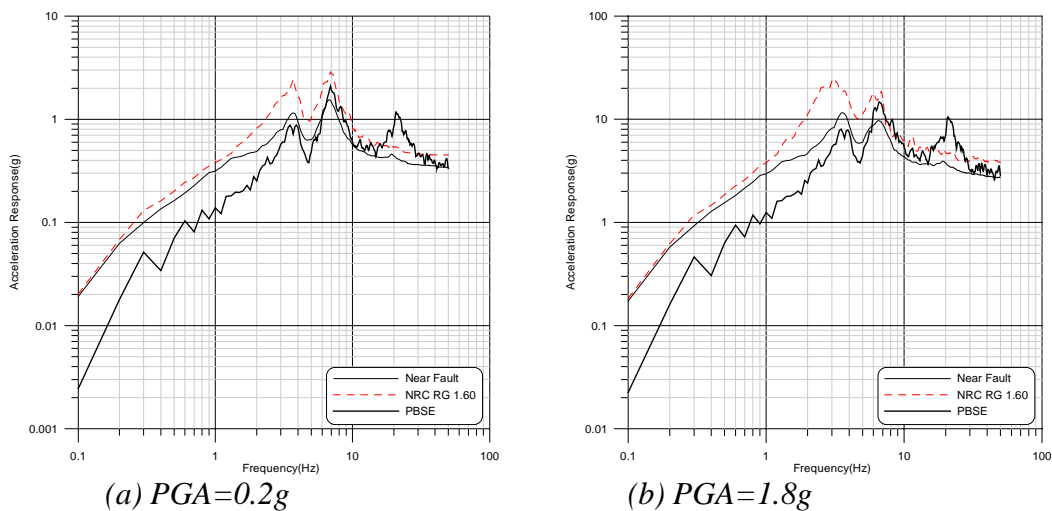
The seismic responses of the structure were investigated in the above section. Based on the analysis results, it seems that the design earthquake for the Korean nuclear power plants is conservative, because the fundamental frequency of the major nuclear power plant structures is greater than 4Hz. From the structural point of view, the containment building has enough safety margins for the earthquake ground motions. In nuclear power plant structures, many kinds of equipment important for its safety are installed on the floor or wall with a welded or bolted anchorage. The dynamic characteristics of those equipments are various. And the failure mode due to an



earthquake is composed of the structural failure mode and the functional failure mode. The structural failure mode, such as an anchorage failure, is mainly dominated by the global modal response of the structures. The functional failure mode is dominated by the local response of the equipment. It is noted from the fragility analyses performed for the probabilistic seismic risk assessment that the dominant failure mode of the active components is a functional failure due to the chattering of the relay attached to the electrical equipment mounts, such as a panel, rack or cabinet (KAERI, 2001).

In general, the relay chattering is very sensitive to the high frequency ground motions (EPRI, 1993). The local vibration mode of the panel induces the high frequency response of the panel. In this study, the floor acceleration response was estimated by using the floor acceleration response spectra. The floor response spectrum is used for the design of the components installed in a building structure. Figure 15 shows the floor response spectra at the top of the containment building. As shown in this figure, the difference of the spectral amplitude increases with an increase of the frequency. The floor response spectra due to the PBSE show high amplitude in the high frequency range greater than 15 Hz.

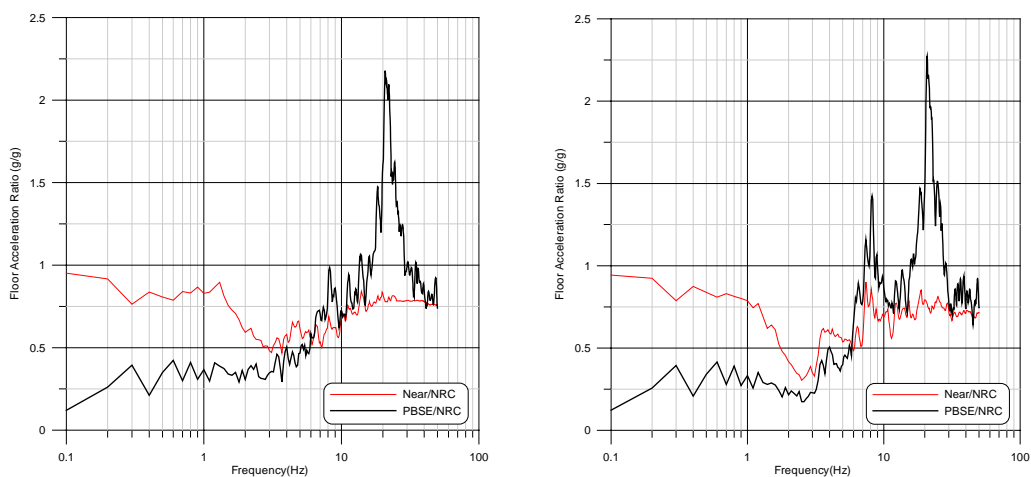
Figure 16 shows the floor acceleration response spectrum ratio. The spectral acceleration induced by the PBSE in the high frequency region is greater than induced by the NRC ground motion. It means that the PBSE can affect the safety of the safety related equipment sensitive to the high frequency ground motions. The near fault ground motion is not so damaging for the equipment which have high natural frequency.



(a)  $PGA=0.2g$

(b)  $PGA=1.8g$

Fig. 15 Floor Acceleration Response Spectrum at Top



(a)  $PGA=0.2g$

(b)  $PGA=1.8g$

Fig. 16 FRS Ratio of the Containment Building at Top



## 5. CONCLUSIONS

In this study, inelastic nonlinear seismic analyses of the CANDU containment building were performed to estimate the seismic response for the design ground motion and several near-field ground motions.

The CANDU containment building shows a nonlinear behavior for the NRC design ground motion greater than 0.6g PGA. The displacement responses due to the near-field ground motions were smaller than those due to the NRC design ground motion. This result shows that the PBSE and the near fault ground motion effects are not so damaging to the containment which is a relatively stiff structure, such as the containment building. The containment building shows an elastic behavior for various earthquake ground motions at the SSE (Safe Shutdown Earthquake) level of a PGA.

An active component installed in the NPP structure is generally very sensitive to the high frequency ground motions. The earthquake ground motions recorded in Korea show very rich high frequency contents. The floor acceleration response spectrum induced by the PBSE is greatly amplified in the high frequency region, since the spectral shape of the PBSE also has rich high frequency contents. It means that the characteristics of the PBSE should be considered to secure the seismic safety of the safety related components installed in NPP structures.

In the seismic fragility analysis for the probabilistic seismic safety assessment, the seismic safety of the NPP structures is estimated based on the stress response. It is not enough to estimate the seismic safety of a structure by a stress response. The displacement response is a very important factor for the seismic safety of a structure. The displacement based seismic fragility analysis is essential to estimate the seismic margin of the containment building when considering the nonlinear dynamic behavior.

## ACKNOWLEDGEMENT

This research was supported by the Mid- and Long-Term Nuclear Research & Development Program of the Ministry of Science and Technology, Korea.

## REFERENCES

- CANATOM (1994), Wolsung 2 Nuclear Power Plant – Design Report for Reactor Building Containment Structure Stress Analysis, 8602-21020-0002-00-DR-A.
- Choi, In-Kil, Young-Sun Choun, and Jeong-Moon Seo(2003), “Scenario Earthquakes for Korean Nuclear Power Plant Site Considering Active Faults”, SMiRT-17, Prague, Czech Republic, August 17-22, 2003.
- Electric Power Research Institute (1993), Analysis of High-Frequency Seismic Effects, EPRI TR-102470
- KINS (2000), Development of Seismic Safety Evaluation Technology for NPP Sites, KINS/GR-206, 2000.
- Korea Atomic Energy Research Institute (2001), External Event Analysis Based on Probabilistic Approaches, KAERI/CM-574/01.
- NRC (1973), US NRC Regulatory Guide 1.60, Design Response Spectra for Seismic Design of Nuclear Power Plants, 1973.
- NRC (1997), US NRC Regulatory Guide 1.165, Identification and Characterization of Seismic Sources and Determination of Safe Shutdown Earthquake Ground Motion.
- Ohno, S., M. Takemura, and Y. Kobayashi, “Effects of Rupture Directivity on Near-Source Strong Motion,” Proc. 2<sup>nd</sup> International Symposium on the Effects of Surface Geology on Seismic Motion, 1998.
- Park, Y. J. and C. H. Hofmayer(1994), Technical Guidelines for Aseismic Design of Nuclear Power Plants, Translation of JEAG 4601-1987, NUREG/CR-6241, 1994.
- Seo, Jeong-Moon, Gyung-Shik Min, Young-Sun Choun, and In-Kil Choi (1999), Reduction of Uncertainties in Probabilistic Seismic Hazard Analysis, KAERI/CR-65/99.
- Vanmarcke, E.H., C.A. Cornell, D.A. Gasparini, and S.N. Hou (1976), SIMQKE : A Program for Artificial Generation User’s Manual and Documentation, Department of Civil Engineering, MIT.